Published paper

Beck, S.B.M., Bagshaw, N.M. and Yates, J.R. (2005) *Explicit equations for leak rates through narrow cracks.* International Journal of Pressure Vessels and Piping, 82 (7). pp. 565-570.

http://dx.doi.org/10.1016/j.ijpvp.2004.12.005

Explicit equations for leak rates through narrow cracks

S.B.M. Beck, N.M. Bagshaw[1] and J.R. Yates

Department of Mechanical Engineering, The University of Sheffield, Mappin Street, Sheffield, UK, S1 3JD

ABSTRACT

Explicit equations to describe the leak rate of a single phase fluid through a narrow crack under a low pressure gradient have been developed and are presented. Four distinct flow regimes, which change with crack opening displacement, have been previously identified and are the basis of this model. The fluid flow is governed by the pressure gradient and the tortuosity of the crack, which is particularly important when the opening displacement is small.

The equations have been developed by considering the pressure forces created when the fluid flows down an idealised zig-zag channel. The nature of the flow, and hence the governing equations, change as the crack aperture increases.

The power of this approach is clearly seen when the flow rates predicted using this model are compared both to the flow rates predicted from computational fluid dynamics analyses and those found by experimentation. The agreement between these sets of data is good, showing that the major effects governing the flow rate have been identified and accounted for.

Keywords: Cracks, Flow, Leak before break, Explicit equations, single phase

[1] Now at TWI, Abington, Cambridge., UK

NOMENCLATURE

A	Flow area
C_d	Discharge coefficient
d	Hydraulic diameter or mean crack width
f	Friction factor
G	Gap between the tips of the crack surfaces
l	Wall thickness of structure and hence depth of crack
ℓ	length of arc of flow around crack tip
N	Number of grain faces along the crack surface
ΔP	pressure difference over a length ℓ
$\dot{Q}$	Volumetric flow through crack
r	radius of curvature of flow around crack tip
Re	Reynolds number = $\frac{\rho v d}{\mu}$
u	Mean velocity of the flow.
ε	Perpendicular height of grain
μ	Fluid viscosity
ρ	Fluid density
θ	half angle of curvature (full angle = 2θ)

SUBSCRIPTS

e	Expansion
eff	Adjusted flow channel dimensions
i	Inertia pressure
μ	Viscosity

1 INTRODUCTION

The detection of pressure loss or fluid leakage from a cracked pressure vessel is a key part of a leak-before-break (LBB) safety assessment. In principle, there are two stages to LBB failure assessment procedures. The first is to estimate the size of through wall crack that would leak at a given rate under normal operating conditions. The second is to determine whether such a crack, with an acceptable factor of safety, would remain stable under any conceivable extreme load case. There are further important, detailed aspects to LLB analyses associated with the growth of part, or fully penetrating cracks; These will not be dealt with here, but information and data on all aspects of leak before break, including crack growth are very well covered in various reports [1, 2].

Much of the published research effort in measuring and calculating leak rates has focussed on high pressure fluids leaking through relatively wide open cracks in thick walled vessels. The studies reported in this paper have been directed at exploring single phase fluid flow through narrow cracks in low pressure, thin walled structures.

Recent work in this area by Rudland and Wilkowski [3,4] suggests that failure probabilities are more sensitive to the leak rate analysis than the fracture analysis. In an early paper, Matsushima *et al*. [5] described measurements of leak rates of high pressure saturated water through flat orifices and rectangular slits with artificially roughened surfaces. They concluded that leak rates are influenced by loading stress, crack opening displacement, surface roughness and the exit to stagnation area ratio of the leak flow path.

Chivers [6] described a model for leak rates through cracks based on a length and a friction factor. The factor was derived from an empirical relationship found from experiments on roughened plates. Two flow regimes, one laminar and one turbulent, were identified and are accounted for in the friction factor. The tortuosity of the crack was accounted for by varying its length. Bagshaw *et al*. [7] and Rudland *et al*. [3] have both identified that the length of the flow path, incorporating the number of turns or deviations, is an important parameter. This additional path length is supplementary to conventional measurements of surface roughness and crack morphology.

Fundamental to the approach taken in this work is the existence of four different flow regimes. These describe the increase in fluid flow and a decrease in tortuosity with increasing crack opening displacement. The first two of these regimes were identified by Clarke *et al.*, [8] who categorised them into those dominated by viscous and minor losses respectively. The second of these regimes was then subdivided by Bagshaw *et al.* [7] into one where the flow is forced to follow the profile of the crack, and another where the crack is wide enough for a straight channel to open up for the fluid. As the crack is widened further, or the driving pressure is increased, the inertial forces begin to dominate the minor loss and viscous terms. This is the fourth, turbulent flow, regime and has been known about for a long time [6]. The first and second regimes are highly and fairly tortuous respectively, whereas in the third and fourth the length of the crack path is equal to the thickness of the pressure vessel or pipe wall.

For those interested in a more comprehensive introduction to the subject of flow rates through cracks, the recent papers of Chivers [6] and Xie [9] provide an excellent summary.

2 Fluid flow through narrow cracks with a high tortuosity.

During leakage, fluid is forced through a crack by a pressure difference existing across the wall of a pipe or pressure vessel. The rate at which the fluid exits the crack, however, depends on how the pressure forces are exerted, or in other words, how the pressure is dissipated across the pressure gradient. An idealized crack is shown in figure 1. The pressure is lost through the crack by three means: viscosity, inertia pressure and the expansion of the fluid, as shown in Equation (1).

$$\Delta P = \Delta P_v + \Delta P_i + \Delta P_e \quad (1)$$

The Poiseuille equation of laminar flow through parallel planes only considers viscosity as a means of resistance to the motion of the fluid. Our analytical model accounts for the pressure losses of viscosity by accommodating the equation shown in equation (1) with the appropriate geometry of flow area, according to the relationships between opening and surface roughness as described above in [6 and 7]. In equation (1), ΔP_v represents the pressure loss due to the effect of viscosity, ℓ_{eff} and d_{eff} are adjusted using flow channel dimensions (see figure 2 (a and b)) to produce equation (2).

$$\Delta P_v = \frac{12\mu \ell_{eff} u}{d_{eff}^2} \quad (2)$$

Forces act on fluid bodies when the flow is undergoing accelerations. These forces are associated with a pressure gradient for which the difference is sometimes known as the inertia pressure. In this case, the effect of inertia pressure losses within the idealised crack arises due to the fluid accelerating around the corners of the crack asperities. Equation (3) describes the inertia pressure loss [10]. The inertia force is given by the product of the mass of the fluid and the acceleration around a crack tip having a radius, r, and an arc length, ℓ.

$$\Delta P_i A = A \frac{\rho u^2}{2} \frac{\ell}{r} \quad (3)$$

The distance of the accelerating flow was assumed to be the product of the angle of curvature, which equals 2θ (radians), and the radius. Therefore, in two dimensions the area is simply the effective crack opening displacement and Equation (4) gives the inertia force that exists across the crack. In the equation, N represents the number of grain faces, or crack facets along the crack surface. See Figure 3 for the notation of the symbols used.

$$P_i d = N d_{eff} \frac{\rho u^2}{2} 2\theta \quad (4)$$

The tortuosity of crack profiles results in flow separation from the surfaces of the crack. Part of the fluid flows into the regions of low pressure created by the separation. In these regions the fluid behaviour is turbulent. The flow is re-circulated producing vortices, or eddies. The expansion of the fluid in these regions causes a reduction in pressure within the fluid. The magnitude of the loss for each grain is related to the area of re-circulated flow and is estimated by Equation (5) which is the standard equation for the pressure loss in a sudden expansion [10] multiplied by the number of crack facets.

$$\Delta P_e = N \frac{\rho u^2}{2} \left(1 - \left(\frac{d_{eff}}{d}\right)^2\right) \quad (5)$$

As only two dimensions are considered, it is straightforward to obtain the geometrical crack opening variables d_{eff} and d.

~~1.5~~Correction for surface roughness

Formatted: Bullets and Numbering

For crack openings smaller than the scale of the surface roughness, the fluid is forced to flow around the peaks of the crack asperities. For these crack openings the effect of expansion is assumed to be negligible since the amount of re-circulated flow is minimal. Setting P_E to zero in Equation 1 gives Equation (6), the pressure difference across the crack.

$$\Delta P = \Delta P_v + \Delta P_i \tag{6}$$

For this condition, the pressure difference forcing the fluid to flow through the restricted channel of δ_{eff} will be the same value for P_i and P_v (see fig 2). Therefore, equating the pressure terms to give the velocity and subsequently substituting the velocity into the pressure terms of Equation (6) gives an estimated effective flow area as shown below in Equation (7).

$$\delta_{eff} = \left[\frac{2}{\Delta P}\frac{2(12\mu\ell_{eff})^2 d}{N\rho 2\theta}\right]^{0.2} \tag{7}$$

The angle, 2θ, in Equation (6) results from the fluid travelling 90° around each grain corner, and the effective length is the combined lengths of all the crack faces. When a gap develops between the tips of the crack profile, the effective flow area follows an angle of curvature given by Equation (8).

$$\theta = \tan^{-1}\frac{(d_{eff} - G)}{d_{eff}} \tag{8}$$

The flow travels a distance ℓ_{eff} which is shown in Equation (9).

$$\ell_{eff} = N\varepsilon\cos\theta \tag{9}$$

When the effective flow area is of the same magnitude as the gap between the asperity tips of the crack surfaces, G, see Figure 3, θ tends to zero and the effective length tends to the direct through-wall length of the crack. The fluid now travels directly through the crack, in the gap between the asperities. Equation (10) shows all the pressure terms expanded.

$$\Delta P = \frac{12\mu\ell_{eff}u}{d_{eff}^2} + N\frac{\rho u^2}{2}2\theta\frac{d_{eff}}{d} + N\frac{\rho u^2}{2}\left(1-\left(\frac{d_{eff}}{d}\right)^2\right) \tag{10}$$

Rearranging Equation (10) gives Equation (11) and shows that a quadratic equation exists from which the velocity u can be obtained.

$$0 = \frac{\rho u^2}{2}\left[N2\theta\frac{d_{eff}}{d} + N\left(1-\left(\frac{d_{eff}}{d}\right)^2\right)\right] + \frac{2u}{\rho}\left[\frac{12\mu\ell_{eff}}{d_{eff}^2}\right] - \Delta P \tag{11}$$

The volumetric leak rate through the crack is the product of velocity and area, $\dot{Q} = ud_{eff}$, where $\dot{Q}$ is the flow per unit surface crack length.

1. For narrow (thin) cracks, the flow is dominated by the viscosity.

$$0 = \frac{2u}{\rho}\left[\frac{12\mu\ell_{eff}}{d_{eff}^2}\right] - \Delta P \tag{12}$$

2. as the crack gets larger, the flow goes through a less tortuous route curving between the tips of the asperities, the inertia pressure becomes more important, though the viscous

forces cannot be ignored.

$$0 = \frac{\rho u^2}{2}\left[N 2\theta \frac{d_{eff}}{d}\right] + \frac{2u}{\rho}\left[\frac{12\mu\ell_{eff}}{d_{eff}^2}\right] - \Delta P \qquad (13)$$

3. Once the crack opens still further, the expansions and contractions start to account for much of the flow, though the pressure loss due to the viscosity is still present. The inertia forces are now very minor as θ tends to zero.

$$0 = \frac{\rho u^2}{2}\left[N\left(1-\left(\frac{d_{eff}}{d}\right)^2\right)\right] + \frac{2u}{\rho}\left[\frac{12\mu\ell_{eff}}{d_{eff}^2}\right] - \Delta P \qquad (14)$$

4. At the pressure increases, the flow becomes turbulent, and the pressure loss is based on the expansions and contractions. The other terms become relatively unimportant.

$$0 = \frac{\rho u^2}{2}\left[N\left(1-\left(\frac{d_{eff}}{d}\right)^2\right)\right] - \Delta P \qquad (15)$$

These equations can be used to predict fluid flow rates from crack opening displacements and the pressure drop through the pressure vessel or pipe wall.

Formatted: Bullets and Numbering

~~2~~3 Comparison with experimental results

To assess the analytical model described above, both computational and experimental data that had previously been produced by the Sheffield group [7] were plotted against values that were estimated for the model. The parameters that are used in the model include: the density and viscosity of the fluid; the pressure difference across the crack; the vertical and horizontal dimension of the surface roughness; the number of faces along the crack surface; and the crack opening displacement.

The geometry shown in Figure 1 was initially used to model the conditions for the idealised two-dimensional CFD models whose characteristic roughness was 31μm. Water was driven through the cracks by a pressure gradient of 29 MPa m^{-1}. The results of this analysis are shown in Figure 4.

To assess the model at higher Reynolds numbers, the model was also tested against the conditions of a second CFD model of a larger (though still idealised) crack, with flow conditions that yielded a Reynolds number an order of magnitude greater than the first CFD model. In this case, air was driven through the cracks by a pressure difference of 3200 Pa m^{-1} applied across the crack (Figure 5). Leak rates were recorded through crack openings up to twice the surface roughness, which was 2.78 mm. The flow conditions through these cracks had Reynolds numbers that were in the order of 1000. Air and water flow experiments were also performed as part of previous work [7]. Figure 6 shows both the experimental and CFD results using air plotted along with the associated results from the model described above.

Figure 7 shows the influence of pressure gradients and crack opening on the flow through the crack. Figure 8 shows the effect on the flow rate of altering the angle of the facets on the crack surface.

Formatted: Bullets and Numbering

~~3~~4 DISCUSSION

The analysis described in this paper is intended to be used for single phase flow under laminar, isothermal conditions. The crack fracture surfaces are assumed to be parallel and coincident.

The method tends to give an underestimate of the maximal flow through the crack under these conditions. In other words, an experimentally measured flow will indicate an opening that will be larger than the physical dimensions of the crack. However, when the crack faces are displaced relative to each other, or when the crack faces converge, or when other obstructions are present, the actual flow rate will be reduced and the model will underestimate the size or opening displacement of the crack.

This single phase, isothermal, model is suitable for liquids and gases, providing it is appreciated that for very high pressures, the expansion will overcome the limitations of the laminar flow regime and the fluid may cool down as it expands.

The importance of this work is that the use of the leak rate prediction tools in BS7910 [2] with crack opening displacements of less than 150 μm will, on some occasions, overestimate the fluid leak rate and on other occasions underestimate the leak rate. The errors, compared with the new model, can be in excess of a factor of five.

The parameter that is the most crucial, and that one that is hardest to ascertain is the characteristic roughness of the fracture surface. Ideally, this will be known or measured and can be input into the analysis. If it is not known, a value appropriate to the failure mechanism should be used. In the case of intergranular fracture the grain size would be suitable. Guidance of typical surface roughness values for various failure mechanisms is given in Table IV.5.3 of the SINTAP report [**Error! Bookmark not defined.**]. The other parameter that is to be considered is the characteristic angle θ. This will be seen to have the greatest effect at small crack openings. Comparison with experimental results indicates that in the absence of proper measurement, a value of 30° is reasonable.

The exact selection of these parameters appears not to be critical. Using the factors enumerated above will provide results that are consistent with experimental data. Either measurement or experience will allow the user to use optimum values for their particular application.

Evidence to date suggests that the macroscopic tortuosity, as the crack path wanders, is much less significant than the microscopic tortuosity arising from the fracture process, provided that the crack faces remain coincident.

5 CONCLUSIONS

A new method of modelling single phase flow through narrow cracks has been shown to produce good results, and has been compared to a variety of published experimental and computational results. The work both builds upon, and shows the value of, the four flow regimes described in previous work.

The implications of these findings are extensive. For instance, the effective flow area of a long, narrow, wall penetrating crack is very much smaller than might be expected. The regions close to the crack tip have very low flow rates and the leak rate is dominated by the central, wide open portion of the crack. In cases where the crack is under membrane and bending stresses, the region where the crack is narrowest will determine the leak rate.

More work needs to be conducted into the modelling of three dimensional flow in cracks to further understand the implication of the tortuosity on this type of flow. This will then either show the robustness of the model described above or indicate what additional terms need to be developed to allow modelling of the more general case.

6 ACKOWLEDGEMENTS

The authors wish to thank the HSE for funding this work, and the input from Mr H Bainbridge.

7 REFERENCES

1 SINTAP: Structural Integrity Assessment Procedures for European Industry, Project BE95-1426. Final Procedure, British Steel Report, Rotherham, 1999.

2 BS 7910:1999, Guide on methods for assessing the acceptability of flaws in metallic structures, British Standards Publishing Limited (BSPL), 1999.

3 Rudland, D.L., Wilkowski, G. and Scott, P., Effects of crack morphology parameters on leak-rate calculations in LBB evaluations. International Journal of Pressure Vessels and Piping, **79**, 2, 99-102, 2002.

4 Rudland, D.L., Wang, Y.-Y. and Wilkowski, G., Comparisons of crack opening displacement predictions for LBB applications. International Journal of Pressure Vessels and Piping, **79**, 202-217, 2002.

5 Matsushima, E., Yano, T. and Okamota, A., Evaluation of leak flow rate and jet impingement related to Leak-Before-Break, Nuclear Engineering and Design, **111,** 197-205, 1989.

6 Chivers, T.C., The influence of surface roughness on fluid flow through cracks, Fatigue and Fracture of Engineering Materials and Structures, **25**, 11, 1095-1102, 2002.

7 Bagshaw, N.M., Beck, S.B.M. and Yates, J.R., Fluid flow rates through thin cracks. Proceedings of the Institution of Mechanical Engineering, **214** Part C, pages 1099-1106, 2000

8 Clarke, L.V., Bainbridge, H., Beck, S.B.M. and Yates, J.R., An investigation into fluid flow rates through cracked plates. International Journal of Pressure Vessels and Piping, **71**, 71-75, 1997.

9 Xie, L. and Yu, Z., A probabilistic simulation of fluid leakage in multiple cracks situation. Fatigue and Fracture of Engineering Materials and Structures, **25**, 11, p 1087-10942002.

10 Massey, B.S., Mechanics of Fluids. Chapman & Hall, 6th edition, 1989.

List of figures

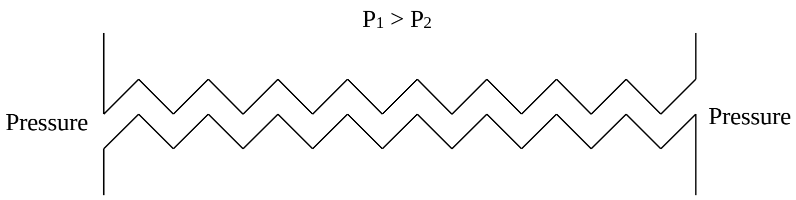

Figure 1: Geometry of an idealised crack

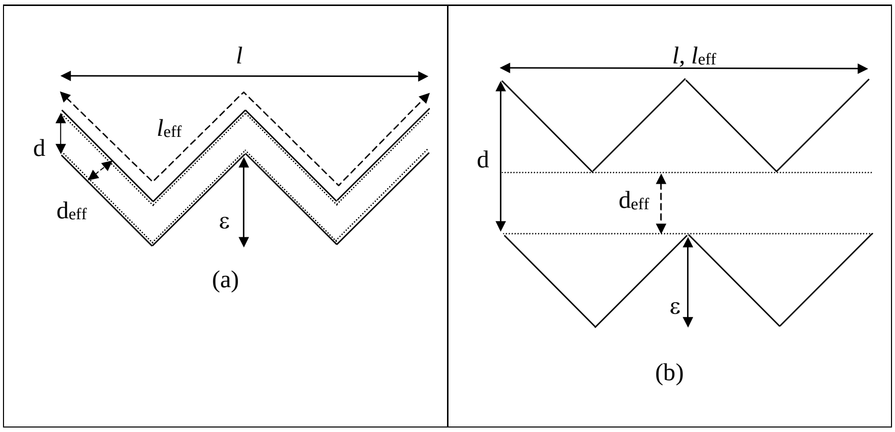

Figure 2: Effective flow areas for different crack openings

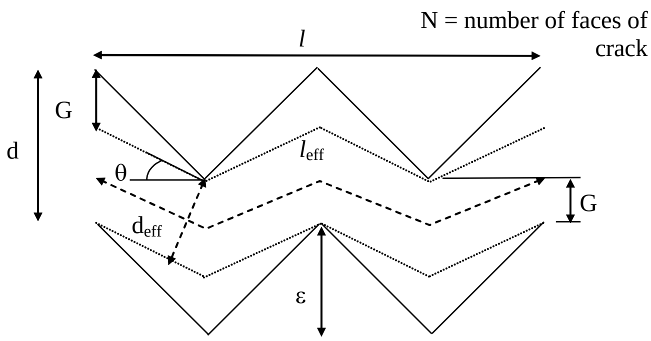

Figure 3: Section of the idealised crack showing the effective flow area

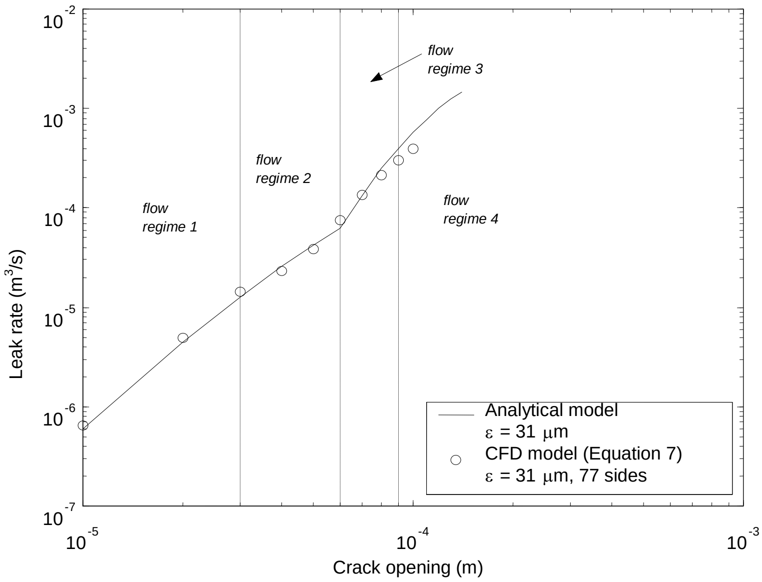

Figure 4 Water leak rates plotted against crack opening for analytical and computational models (pressure gradient of 29 M Pa m^{-1} applied across the cracks).

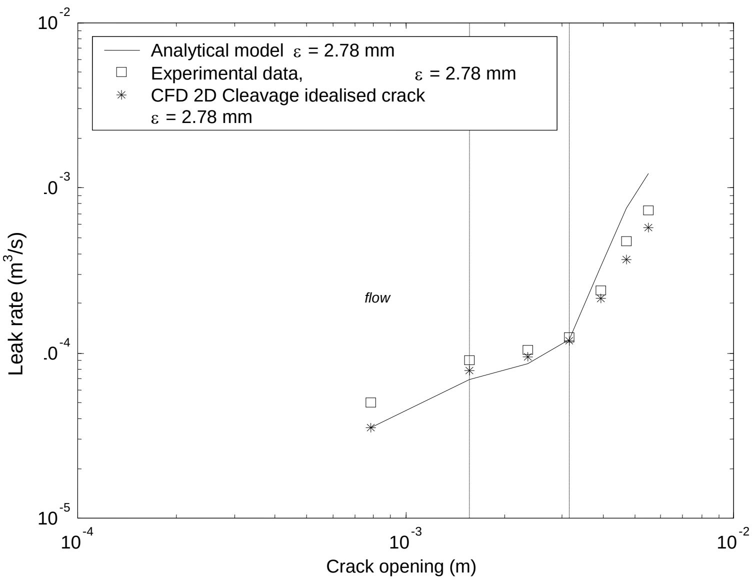

Figure 5 Water leak rates plotted against crack opening for large scale analytical and computational models. (pressure gradient of 3200 Pa m^{-1} applied across the cracks)

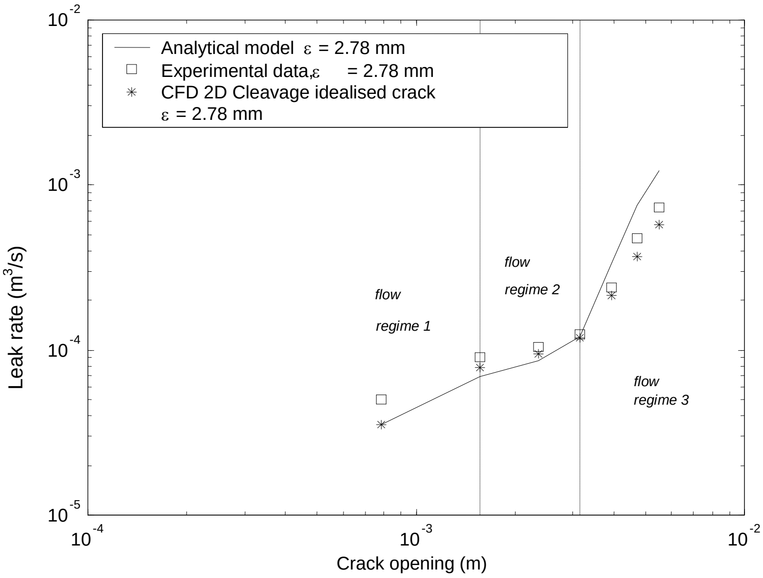

Figure 6 Air leak rates plotted against crack opening comparing the analytical model with the experimental and computational idealised crack (pressure gradient of 1560 Pa m^{-1} applied across the cracks).

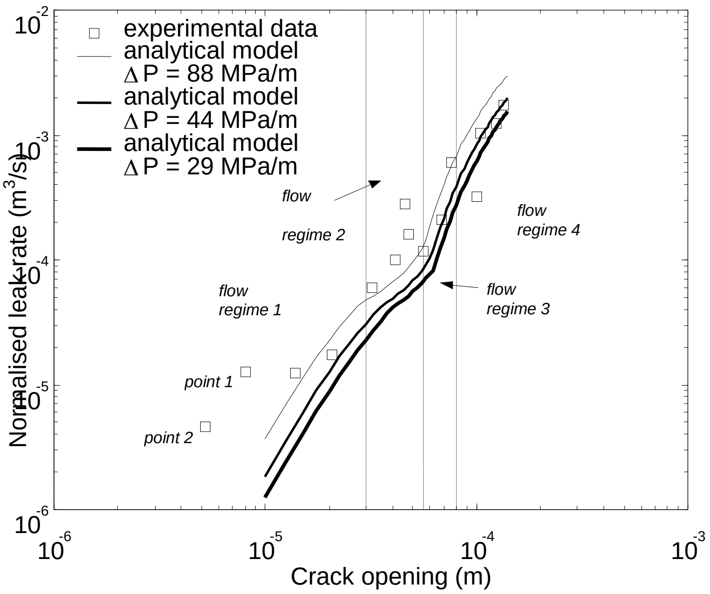

Figure 7 Analytical solutions of leak rates compared with experimental data.

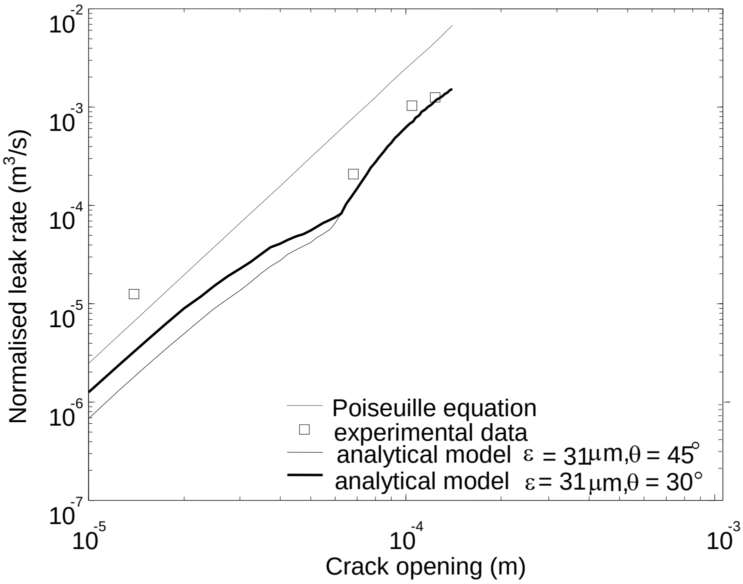

Figure 8 Water leak rates through crack openings for a pressure gradient of 29 MPa m^{-1}.